Scientific paper

Synthesis, Crystal Structures, Molecular Docking and MAO-B Inhibitory Activity of Transition Metal Complexes Derived from 2-(4-(Pyridin-2-yl)piperazin-1-yl)acetic Acid

Yan-Jie Ren, Jin-Long Zhu, Li-Xin Zhang, Yin-Xiang Xu and Shao-Song Qian*

School of Life Sciences, Shandong University of Technology, Zibo 255049, P. R. China

** Corresponding author: E-mail: sdutqianss@163.com*
Tel.: 0086-533-2780271; Fax: 0086-533-2781329.

Received: 22-02-2017

Abstract

Three new complexes derived from 2-(4-(pyridin-2-yl)piperazin-1-yl)acetic acid (**HL**), $[M(\mathbf{L})_2(H_2O)_2]$ where M = Cu^{II} (**1**), Zn^{II} (**2**) and Cd^{II} (**3**), have been synthesized and characterized by IR spectroscopy, elemental analysis and X-ray crystallography. The inhibitory activity of these three complexes against MAO-B was tested *in vitro*, and the molecular docking experiments were also carried out to rationalize their binding models. Both the experimental and docking simulation results indicated that complex **1** has the best inhibitory activity with IC_{50} value being 6.5 ± 0.31 μM.

Keywords: Metal complexes, Crystal Structure, MAO-B inhibitor; Molecular Docking

1. Introduction

Monoamine oxidases (MAOs, EC 1.4.3.4) are well known enzymes bound to the outer membrane of mitochondria through a C-terminal transmembrane helix and catalyze the oxidative deamination of monoamine neurotransmitters in the central nervous system.[1–3] MAOs occur in two forms designated as MAO-A and MAO-B, which have different substrate preference and inhibitor specificity.[4,5]

An increase of the dopamine levels as well as a neuroprotective effect can be observed following the inhibition of MAO-B.[6] Therefore, MAO-B inhibitors can be used to treat the neurodegenerative disorders such as Aizheimer's disease (AD) and Parkinson's disease (PD).[7–9] Kinds of heterocyclic scaffolds such as chalcone,[10] coumarin,[11] pyrazoline[12] and oxadiazole[13] derivatives have been demonstrated as MAO-B inhibitors. Recently, pyridoxine-resveratrol hybrids Mannich base derivatives have been reported as MAO-B inhibitors by Yang et al.[14]

As mentioned above, most reported MAO-B inhibitors are organic heterocyclic molecules while MAO-B inhibitors based on metal complexes are seldom discussed. In our earlier work, we investigated the urease inhibitors and the MAO-B inhibitory activity of metal complexes.[15,16] The inhibitory activities of these bioactive complexes are affected by the central metal and the coordination modes of the ligand. As a continuation of our study, in this paper, three new complexes $[M(\mathbf{L})_2(H_2O)_2]$ where M = Cu^{II} (**1**), Zn^{II} (**2**) and Cd^{II} (**3**), were obtained derived from 2-(4-(pyridin-2-yl)piperazin-1-yl)acetic acid (**HL**) and corresponding metal nitrates. Herein, the synthesis, characterization, MAO-B inhibitory activity and molecular docking are presented.

2. Experimental Section

2. 1. Materials and Methods

All chemicals and solvents were analytical reagent grade and purchased from Aladdin Industrial Corporation (China). They were used without purification. Elemental analyses for C, H, and N were conducted using the Pregl-Dumas technique on a Thermo Fischer Flash EA1112. FT-IR spectra were recorded from 400–4000 cm^{-1} on a Nicolet 750 Magna IR spectrometer using KBr pellets. The enzyme inhibitory activity was measured on a Bio-Tek Synergy™ HT Microplate reader.

2. 2. Synthesis of 2-(4-(pyridin-2-yl)piperazin-1-yl)acetic Acid (HL)

HL was prepared according to the method reported with suitable modification.[17,18] 1-(pyridin-2-yl)piperazine (1.00 g, 0.0060 mol), bromoacetic acid (2.50 g, 0.0179 mol), and potassium hydroxide (1.50 g, 0.267 mol) were dissolved in 30 mL absolute ethanol. The mixture was refluxed for 10 h. When the reaction was finished, the solution was cooled to room temperature and neutralized with 1 M HCl. White precipitate was filtered to give **HL** (1.01 g, 74%).

2. 3. General Procedure for the Synthesis of Complexes 1–3

Nitrate (0.040 mmol) was dissolved in 4 mL of methanol solution which was carefully layered on the top of 4 mL water solution of **HL** (8.84 mg, 0.040 mmol) and KOH (2.24 mg, 0.040 mmol). The solutions were left for a few days at room temperature and then the crystals were obtained.

$[Cu(\mathbf{L})_2(H_2O)_2]$ (**1**) Yield: 0.0372 g, (43% on the basis of HL). IR (KBr, cm^{-1}): 3365; 2970; 1596; 1467; 1384; 845; 681. Anal. Calcd. for $C_{22}H_{32}N_6O_6Cu$: C, 48.97; H, 5.97; N, 15.56. Found: C, 49.09; H, 5.95; N, 15.56%.

$[Zn(\mathbf{L})_2(H_2O)_2]$ (**2**) Yield: 0.0442 g, (51% on the basis of HL). IR (KBr, cm^{-1}): 3338; 2943; 1595; 1454; 1395; 831; 664. Anal. Calcd. for $C_{22}H_{32}N_6O_6Zn$: C, 48.76; H, 5.95; N, 15.51; Found: C, 48.91; H, 5.92; N, 15.56.%.

$[Cd(\mathbf{L})_2(H_2O)_2]$ (**3**) Yield: 0.0433 g, (46% on the basis of HL). IR (KBr, cm^{-1}): 3359; 2995; 1594; 1458; 1394; 836; 671. Anal. Calcd. for $C_{22}H_{32}N_6O_6Cd$: C, 44.87; H, 5.48; N, 14.27; Found: C, 45.02; H, 5.46; N, 14.29%.

2. 4. X-ray Crystallography

Diffraction intensities for the complexes were collected at 298(2) K using a Bruker D8 VENTURE PHOTON diffractometer with Mo-Kα radiation (λ = 0.71073 Å). The structures were solved by direct methods and refined against F^2 by full-matrix least-squares methods using the SHELXTL-97.[19,20] All non-hydrogen atoms were refined anisotropically, the water H atoms in the complexes were located in difference Fourier maps and refined isotropically with O–H distances restrained to 0.85(1). All other H atoms were placed in idealized positions and constrained to ride on their parent atoms. Details of the crystal parameters, data collection, and refinement are listed in Table 1. The selected bond length and angle data are given in Table 2. The hydrogen bonding data are summarized in Table 3.

2. 5. Rat Brain MAO-B Inhibition Assay

MAO-B was obtained from wista mice with the method that was reported earlier.[21] The content of MAO-B was detected by MU30905 ELISA Kit (details in supplementary

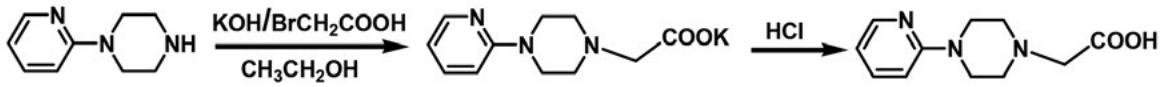

Scheme 1 Synthesis of 2-(4-(pyridin-2-yl)piperazin-1-yl)acetic acid

Table 1. Crystallographic data for complex **1**–**3.**

Empirical formula	1 $C_{22}H_{32}CuN_6O_6$	2 $C_{22}H_{32}N_6O_6Zn$	3 $C_{22}H_{32}CdN_6O_6$
M_r	540.09	541.93	588.95
Crystal system	triclinic	monoclinic	monoclinic
Space group	*P*–1	$P\,2_1/c$	$P\,2_1/c$
a (Å)	6.1916(6)	15.0279(13)	15.0305(14)
b (Å)	8.1504(8)	7.1943(6)	7.2772(6)
c (Å)	12.7804(13)	11.7348(9)	11.8887(10)
α (°)	95.079(3)	90	90
β (°)	103.019(3)	101.273(3)	101.986(3)
γ (°)	106.241(3)	90	90
V (Å^3)	595.33(10)	1244.23(18)	1272.04(19)
Z	1	2	2
ρ_c (g cm^{-3})	1.507	1.446	1.538
F(000)	283.0	568.0	604.0
Data / param. / restr.	2187 / 148 / 0	2202 / 161 / 4	2929 / 157 / 12
μ(Mo-Kα)/ mm^{-1}	0.968	1.036	0.907
GOF	1.108	1.110	1.090
R_1[a], wR_2[b] ($I > 2\sigma(I)$)	0.0663, 0.1684	0.0660, 0.2290	0.0370 , 0.1085

[a] $R_1 = \Sigma||F_o| - |F_c||/\Sigma|F_o|$. [b] $wR_2 = [\Sigma w(F_o^2 - F_c^2)^2/\Sigma w(F_o^2)]^{1/2}$

materials).[22] The MAO-B inhibitory properties of complex **1**–**3** were carried out as it was reported previously.[23]

2. 6. Molecular Docking

Molecular docking of complexes **1**–**3** with the active site of human MAO-B (3LA4) was performed by the AUTODOCK 4.2 program suite. The graphical user interface AutoDockTools (ADT) was performed to setup every inhibitor enzyme interaction, where all hydrogen atoms were added, Gasteiger charges were calculated and non-polar hydrogen atoms were merged to carbon atoms. The result file was saved as pdbqt file. The 3D structures of ligand molecules were saved in Mol2 format with the aid of the program Mercury 3.0. The partial charges of Mol2 file were further modified by using the ADT package (version 1.5.4) so that the charges of the non-polar hydrogen atoms would be assigned to the atom to which the hydrogen is attached. The choice of the flexible bonds in the ligands was in accordance with SP3 hybridization. The nitrogen atoms of ligands in complexes **1**–**3** were assembled as non-protonated. The resulting file was saved as pdbqt file.

The AutoDock Vina docking procedure was used to generate the docking output files.[24] In all docking, a grid box size of 60 × 60 × 60 pointing in *x*, *y* and *z* directions was built, the maps were centered on N5 atom of FAD600.[25,26] A grid spacing of 0.375 Å and a distances-dependent function of the dielectric constant were used for the calculation of the energetic map. Default parameters were used except nummodes, which was set to 10. The results of the most favorable free energy of binding were selected as the resultant complex structures. At the end of the docking, the result was analyzed using Pymol 2.5 program.

3. Results and Discussion

3. 1. IR Spectroscopy

The IR spectra of these complexes were similar. They all show broad band ranging from 3500 cm^{-1} to 3300 cm^{-1} indicating the O–H stretching of the water and methanol molecules. The asymmetric stretching mode $\nu_{as}(COO^-)$ was located around 1595 cm^{-1} (1596 cm^{-1} in **1**, 1595 cm^{-1} in **2** and 1594 cm^{-1} in **3**), while the strong symmetric stretching mode $\nu_s(COO^-)$ for complexes **1**–**3** was clearly visible around 1391 cm^{-1} (1384 cm^{-1} in **1**, 1395 cm^{-1} in **2** and 1394 cm^{-1} in **3**). The separation value $\Delta\nu$ [$\nu_{as}(COO^-) - \nu_s(COO^-)$] of the carboxylic based complexes could be used to discriminate the coordination mode of the carboxyl group. $\Delta\nu < 200$ cm^{-1} indicated the bidentate mode, whereas $\Delta\nu > 200$ cm^{-1} indicated the monodentate mode.[27,28] Therefore, the $\Delta\nu$ values [$\nu_{as}(COO^-) - \nu_s(COO^-)$] for complexes **1**–**3** is around 204 cm^{-1}, which means that the coordination mode of the carboxyl group in these complexes is monodentate.

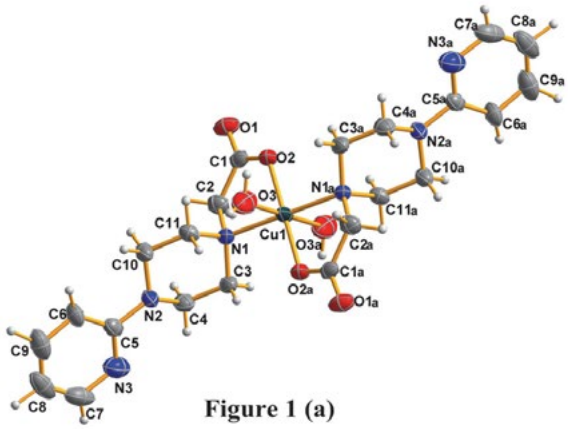

Figure 1 (a)

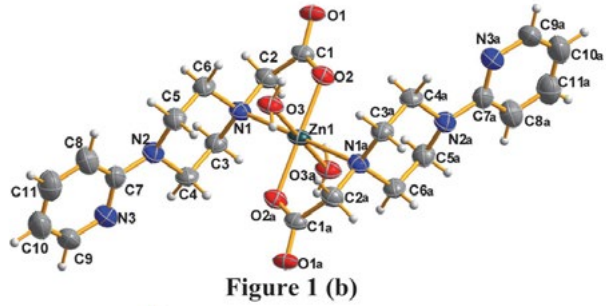

Figure 1 (b)

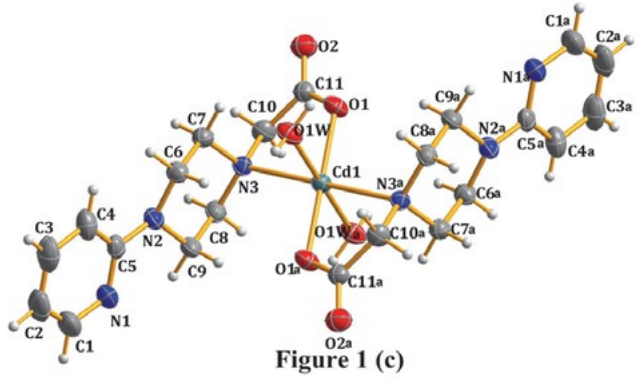

Figure 1 (c)

Figure 1. Molecular structure showing the atom-labelling scheme. Displacement spheres are drawn at the 50% probability level. The molecular diagram of (a) **1**, (b) **2**, (c) **3**.

3. 2. Description of Crystal Structures

Complex **1** crystallizes in triclinic space group *P*–1, while complexes **2** and **3** crystallize in monoclinic space group $P2_1/c$. As shown in Figure 1, these three complexes possess very similar mononuclear structure, so only the structure of **1** is described here in detail. As shown in Figure 1(a), one asymmetric unit contained half of the complex molecule $[Cu(\mathbf{L})_2(H_2O)_2]$. Every mononuclear complex molecule included one copper ion, two ligand molecules and two coordinated water molecules. Ligand **L** behaves as a bidentate ligand resulting in the forming of a novel distorted five-membered heterocyclic ring around copper ion. These two five-membered rings are coplanar. The equatorial plane is surrounded by two O-atom donors (O2 and O2a) and two N-atom donors (N1 and N1a) from two **L** ligands, while the axial positions are occupied by O-atom donors (O3 and O3a) from two coordinated water molecules. In addition, the sum of the equatorial angles N1–Cu1–O2, O2–Cu1–N1a, N1a–Cu1–O2a and O2a–Cu–N1 for complex **1** (= 360.00°) is equal to the ideal value (360.00°), which ensures the planarity of equatorial plane. The axial Cu–O average distance (2.866 Å) is longer than the equatorial Cu–O average distance (2.048 Å) and Cu–N average distance (1.922 Å), showing the stretched tetrahedroid surrounding the Cu(II) center. Compared with the other piperazine-Cu(II) complexes, the Cu–O

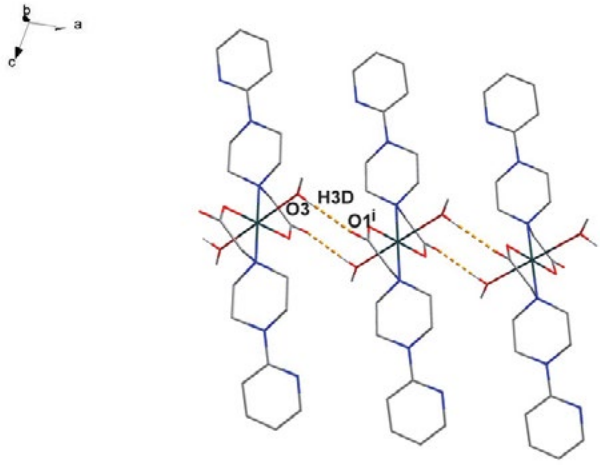

Figure 2. 1-D zig-zag chain of complex **1**. Dashed lines denote hydrogen bonds. Symmetry code: (i) –*x*, 1 – *y*, –*z*.

Table 2. Selected bond lengths (Å) and angles (°) for **1**–**3**

1			
Cu1–O2	1.922(4)	Cu1–O3	2.866(4)
Cu1–N1	2.048(3)		
O2–Cu1–O3	98.30(13)	O2–Cu1–N1	84.33(12)
O2–Cu1–O3a	81.70(13)	O2–Cu1–N1a	95.67(12)
O3–Cu1–N1	93.97(11)	O3–Cu1–N1a	86.03(11)
2			
Zn1–O2	2.006(4)	Zn1–O3	2.107(4)
Zn1–N1	2.362(4)		
O2–Zn1–O3	94.02(14)	O2–Zn1–N1	78.76(13)
O2–Zn1–O3a	85.98(14)	O2–Zn1–N1a	101.25(13)
O3–Zn1–N1	87.95(15)	O3–Zn1–N1a	92.05(15)
3			
Cd1–O1	2.213(2)	Cd1–O1W	2.3055(19)
Cd1–N3	2.456(3)		
O1–Cd1–O1W	94.92(7)	O1–Cd1–N3	74.32(8)
O1–Cd1–O1Wa	85.08(7)	O1–Cd1–N3a	105.68(8)
O1W–Cd1–N3	87.69(8)	O1W–Cd1–N3a	92.31(8)

Symmetry codea: (a) 1 – *x*, 1 – *y*, –*z* for **1**; 1 – *x*, 2 – *y*, 2 – *z* for **2** and 1 – *x*, –*y*, 1 – *z* for **3**.

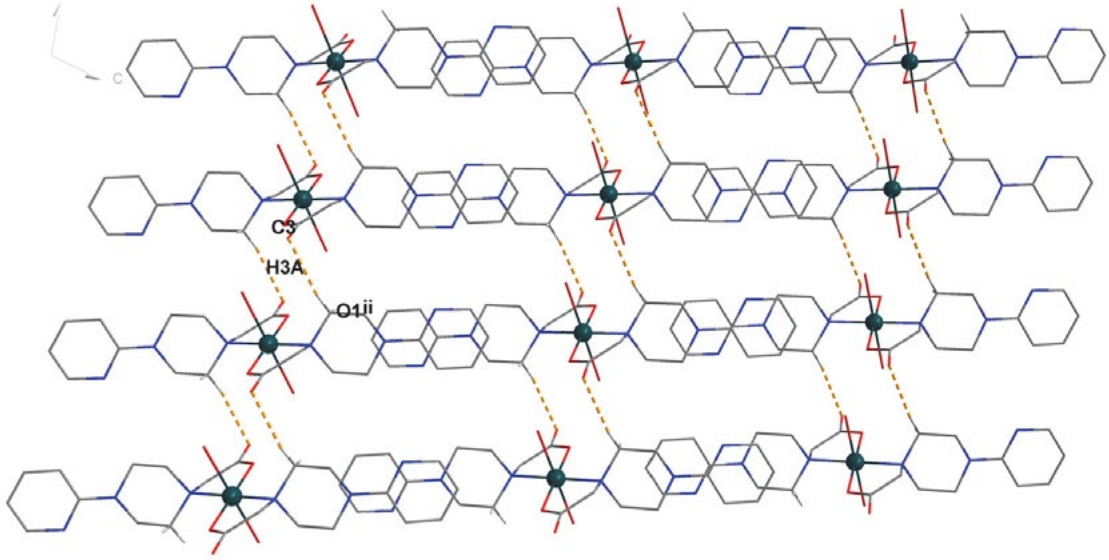

Figure 3. The hydrogen-bond-driven 2D sheet of **1** extended in *bc* plane. Symmetry code: (ii) 1 + *x*, *y*, *z*

Table 3. Geometrical parameters for hydrogen bonds for **1**

Hydrogen bonds	D–H (Å)	H···A (Å)	D···A (Å)	D–H···A(°)
O3–H3D···O1^{i}	0.85	1.96	2.788(5)	164
C3–H3A···O1^{ii}	0.97	2.53	3.476(6)	166

Symmetry codes: (i) $-x$, $1-y$, $-z$; (ii) $1+x$, y, z.

carboxyl bond (1.938 Å) is similar to the Cu–O carbonyl bond length (1.923 Å), and Cu–N bond length (2.033 Å) in complex **1** is also similar to the other piperazine-Cu(II) complexes. The bond distances and bond angles are normal compared to other reported Cu (II) complexes.[29]

Water acts a hydrogen bond donor. As shown in Figure 2, complex **1** presents enhanced hydrogen-bonding framework in the solid state (Table 3). Two coordinated water molecules (O3 and O3a) are involved in a chain formation through O3–H3D1···O1^{i} hydrogen bonding (symmetry code: (i) $-x$, $1-y$, $-z$).

As shown in Figure 3, these chains stack in a interleaved fashion in *bc* plane, the hydrogen bonds exist between the carboxyl group of ligand **L** and the carbon atom of other ligand **L** form intermolecular C3–H3A···O1^{ii} (symmetry code: (ii) $1+x$, y, z)

3. 3. Inhibitory Activity Against MAO-B

Statistical analyses of data were performed using SPSS 19.0 program. Data reported as means ± SEM for three independent samples in duplicate. Statistical differences between the groups were considered significant if the p value was < 0.05. Specific results please see Table **4**. It was found that compared with iproniazid phosphate as the positive control (IP, IC_{50} = 7.59 ± 1.17 μM),[30] complex **1** (IC_{50} = 6.52 ± 0.31 μM) had good inhibitory activity on MA0-B, while complexes **2** and **3** (IC_{50} > 100μM) showed no inhibitory activity. Both $Cu(NO_3)_2$ and ligands have a certain inhibitory capacity for monoamine oxidase, after the two combine to form a complex **1**, complex **1** showed good inhibitory activity, therefore, they show certain synergistic effects.

Table 4. Inhibition of rat brain MAO-B for **HL**, complexes **1–3**, and IP

Test material	IC_{50} (μM)
1	6.52 ± 0.31
2	>100
3	>100
HL	76.1 ± 2.51
$Cu(NO_3)_2$	12.31 ± 1.06
$Zn(NO_3)_2$	>100
$Cd(NO_3)_2$	>100
IP*	7.59 ± 1.17

3. 4. Molecular Docking

The binding models of complexes 1, 2, 3 with MAO-B (1S3E) were simulated using the AutoDock Vina docking program to validate their structure-activity relationships. The docking results show that only the complex **1** has good binding with the active site of MAO-B (1S3E).

The binding model of complex **1** and 1S3E is shown in Figure 4. All amino acid residues around complex **1** are shown. In the binding model, the main stabilizing factors that stabilize the Cu(**L**)$_2$-1S3E complex are the hydrophobic contacts and hydrogen bonding interactions. The O1 atom in complex **1** serves as a hydrogen bond acceptor re-

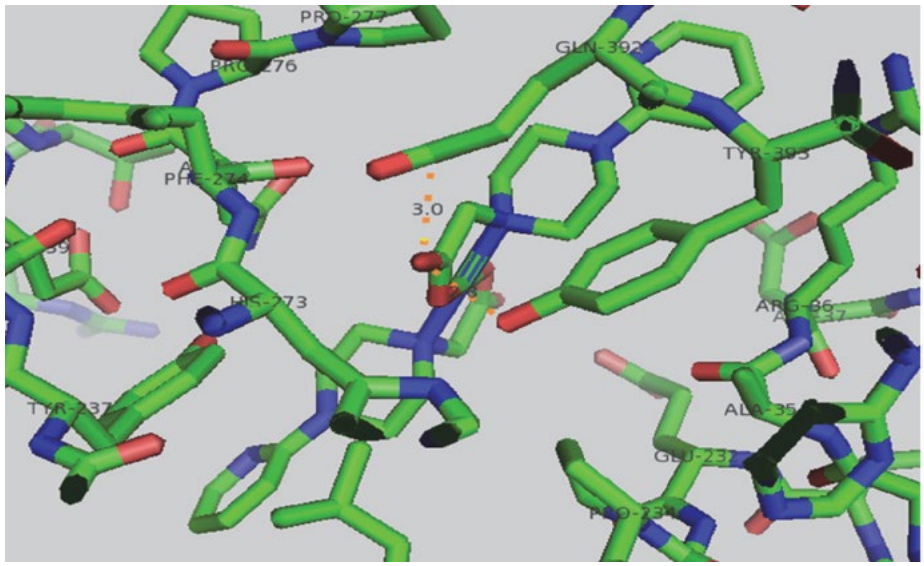

Figure 4. Binding mode of complex **1** with human monoamineoxidase-B. The complex molecule and MAO-B were shown as stick, the hydrogen bonds were shown as yellow dash lines

ceived one strong hydrogen bonding interaction from Tyr393. The hydrogen-bonding distance of Tyr393 N–H···O2 is 2.8 Å. The results of the molecular docking indicate that the complex **1** could be well fitted in the active pocket of MAO-B.

4. Conclusion

This paper reports that synthesis, crystal structure, molecular docking, and monoamine oxidase B inhibitory activities of three transition metal complexes with 2-(4-(pyridin-2-yl)piperazin-1-yl)acetic acid ligand. Molecular docking assay showed the potential binding model of complex **1** with MAO-B. The complex **1** exhibits MAO-B inhibiting activity *in vitro* at micromole concentrations (IC_{50} = 6.5 ± 0.31 μM), whereas complex **2** and **3** exhibits no MAO-B inhibiting activity (IC_{50} > 100 μM). Now, we are synthesizing specific compounds that inhibit the MAO-B based on the complex **1** structure.

5. Supplementary Information

CCDC files 1515965 (**1**), 1515778 (**2**) and 1515777(**3**) contain the supplementary crystallographic data for this paper. These data can be obtained free of charge from The Cambridge Crystallographic Data Centre via www.ccdc.cam.ac.uk/data_request/cif.

6. Referances

1. M. B. Youdim, G. G. Gollins, M. Sandler, *J. Biochem*. **1971**, *121*, 34–36. **DOI:**10.1042/bj1210034P
2. J. C. Shih, *Neuropsychopharmacol.* **1991**, *4*, 1–7.
3. J. W. Greenawalt, C. Schnatiman, *J. Cell. Biol*. **1970**, *46*, 173–179. **DOI:**10.1083/jcb.46.1.173
4. C. W. Abell, S. W. Kwan, *Prog. Nucleic. Acid. Res*. **2001**, *65*, 129–156. http://dx.doi.org/10.1016/S0079-6603(00)65004-3 **DOI:**10.1016/S0079-6603(00)65004-3
5. O. Nakagawasai , Y. Arai , E. H. Satoh, N. Satoh, M. Neda, M. Hozumi, R. Oka, H. Hiraga, T. Tadano, *Neurotoxicology* **2004**, *25*, 223–232. **DOI:**10.1016/S0161-813X(03)00101-3
6. H. P. Volz, C. H. Gleiter, *Drug. Aging* **1998**, *13*, 341–355. **DOI:**10.2165/00002512-199813050-00002
7. J. C. Jean, *Neurotoxicology* **2004**, *25*, 21–30. **DOI:**10.1016/S0161-813X(03)00112-8
8. M. B. Youdim, D. Edmondson, K. F. Tipton, *Nat. Rev. Neurosci.* **2006**, *7*, 295–309. **DOI:**10.1038/nrn1883
9. S. S. Jossan, P. G. Gillberg, C. G. Gottfries, I. Karlsson, L. Oreland, *Nat. Rev. Neurosci.* **1997**, *45*, 1–12. http://dx.doi.org/10.1016/0306-4522(91)90098-9 **DOI:**10.1016/0306-4522(91)90098-9
10. T. Shigeo, Y. Kuwai, M. Tabata, *Planta Med*. **1987**, *53*, 5–8. **DOI:**10.1055/s-2006-962604
11. J. Joubert, G. B. Foka, B. P. Repsold, D. W. Oliver, E. Kapp, S. F. Malan, *Eur. J. Med. Chem*. **2017**, *125*, 853–864. **DOI:**10.1016/j.ejmech.2016.09.041
12. B. Evranos-Aksöz, S. Yabanoğlu-Çiftçi, G. Uçar, K. Yelekçi, R. Ertan, *Bioorg. Med. Chem. Lett*. **2014**, *24*, 3278–3284. **DOI:**10.1016/j.bmcl.2014.06.015
13. S. Distinto, R. Meleddu, M. Yanez, R. Cirilli, G.Bianco, M. L. Sanna, A. Arridu, P. Cossu, F. Cottiglia, C. Faggi, F. Ortuso, S. Alcaro, E. Maccioni, *Eur. J. Med. Chem*. **2016**, *108*, 542–552. **DOI:**10.1016/j.ejmech.2015.12.026
14. X. Yang, X. M. Qiang, Y. Li, L. Luo, R. Xu, Y. X. Z. Zheng, Z. C. Cao, Z. H. Tan, Y. Deng, *Bioorg. Chem*. **2017**, *71*, 305–314. **DOI:**10.1016/j.bioorg.2017.02.016
15. J, Qin, Q. Yin, S. S. Zhao, J. Z. Wang, S. S. Qian, *Acta Chim. Slov*. **2016**, *63*, 55-61.
16. D. D. Yang, R. Wang, J. L. Zhu, Q. Y. Cao, J. Qin, H. L. Zhu, S. S. Qian, *J. Mol. Struct*. **2017**, *1128*, 493-498. **DOI:**10.1016/j.molstruc.2016.08.037
17. C. T. Sadashiva, S. C. J. N. Narendra, K. C. Ponnappa, G. T. Veerabasappa, K. S. Rangappa, *Bioorg. Med. Chem Lett*. **2016**, *16*, 3932–3936. **DOI:**10.1016/j.bmcl.2006.05.030
18. Z. J. Chen, C. N. Xu, J. L. Zhu, D. D. Yang, S. S. Zhao, Y. N. Chen, S. S. Qian, *Acta Chim. Slov*. **2016**, *63,* 165–172. **DOI:**10.17344/acsi.2015.2109
19. G. M. Sheldrick, *Acta Crystallogr. A* **2008**, *64*, 112–122. **DOI:**10.1107/S0108767307043930
20. Bruker, SMART (Version 5.63), SAINT (Version 6.02), SADABS (Version 2.03), Bruker AXS Inc. 2002, Madison,Wisconsin, USA.
21. B. E. Yoon, J. Woo, Y. E. Chun, H. Chun, S. Jo, J. Y. Bae, H. An, J. O. Min, S. J. Oh, K. S. Han, H. Y. Kim, T. Kim, Y. S. Kim, Y. C. Bae , C. J. Lee, *J Physiol.* **2014**, *592*, 4951–4968. **DOI:**10.1113/jphysiol.2014.278754
22. A. Holt, D. F. Sharman, G. B. Baker, M. M. Palcic, *Anal. Biochem*. **1977**, *244*, 384–392. **DOI:**10.1006/abio.1996.9911
23. M. O. Ogunrombi, S. F. Malan, G. T. Blanche, N. Castagnoli, J. J. Bergh, J. P. Petzer, *Bioorg. Med. Chem*. **2008**, *16*, 2463–2472. http://dx.doi.org/10.1016/j.bmc.2007.11.059 **DOI:**10.1016/j.bmc.2007.11.059
24. O. Trott, A. J. Olson, *J. Comput. Chem*. **2010**, *31*, 455–461. **DOI:**10.1002/jcc.21334
25. M. B. Nunez, F. P. Maguna, N. B. Okulik, E. A. Castro, *Bioorg. Med. Chem. Lett*. **2004**, *14*, 5611–5617. **DOI:**10.1016/j.bmcl.2004.08.066
26. L. Santana, H. Gonzalez-Diaz, E. Quezada, *J. Med. Chem*. **2008**, *51*, 6740–6751. **DOI:**10.1021/jm800656v
27. C. T. Sadashiva, J. N. N. S. Chandra, K. C. Ponnappa, G. T. Veerabasappa, K. S. Rangappa, *J. Bioorg. Med. Chem. Lett.* **2006**, *16*, 3932–3936. **DOI:**10.1016/j.bmcl.2006.05.030
28. I. Turel, J. Kljun, *J. Curr. Top. Med. Chem.* **2011**, *11*, 2661–2687. **DOI:**10.2174/156802611798040787
29. H. Y. Luo, J. M. Lo, P. E. Fanwick, J. G. Stowell, M. A. Green, *J. Inorg. Chem.* **1999**, *38*, 2071–2078. **DOI:**10.1021/ic981324f
30. S. S. Xie, X. Wang, N. Jiang, Y. W. Yu, D. G. K. Wang, J. S. Lan, Z. R. Li, L. Y. Kong, *Eur. J. Med. Chem*. **2015**, *95*, 153–165. **DOI:**10.1016/j.ejmech.2015.03.040

Povzetek

Sintetizirali smo tri nove komplekse z 2-(4-(piridin-2-il)piperazin-1-il)ocetno kislino (**HL**), $[M(\mathbf{L})_2(H_2O)_2]$, kjer je M = Cu^{II} (**1**), Zn^{II} (**2**) in Cd^{II} (**3**), ter jih okarakterizirali z IR spektroskopijo, elementno analizo in rentgensko kristalografijo. *In vitro* smo določili inhibitorno aktivnost pripravljenih treh kompleksov proti MAO-B ter izvedli simulacijo molekularnega dockinga za razumevanje načina vezave. Eksperimentalni podatki in računalniške simulacije kažejo, da ima kompleks **1** največjo inhibitorno aktivnost z IC_{50} vrednostjo 6.5 ± 0.31 μM.